

CATHODES

The field of vacuum electronics was launched with the invention of the vacuum tube in 1904. From that time, until the introduction of the transistor in the 1960s, vacuum tubes dominated electronic circuit design. Although solid-state devices have taken over most of modern electronics, there are still a number of important applications in which vacuum tubes play an essential role. Basically, a vacuum tube is an active electronic device that is used to control electron beams for a variety of purposes. Figure 1 shows the essential components of a vacuum tube, the cathode, the anode, and a system of control elements.

Cathodes have been studied extensively, because of their important role in electronic devices. After nearly a century of research and development, cathode design has progressed to a fine art. Cathodes may now be tailored to meet the particular requirements of current, power, stability, brightness, life, beam energy, and frequency modulation for a wide variety of vacuum electronic devices. As technology presses on, new

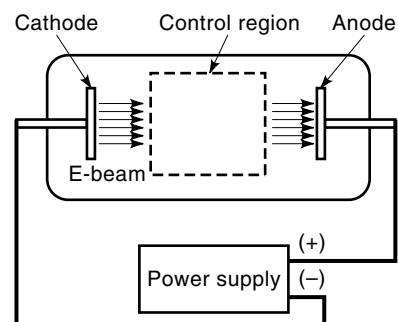


Figure 1. Basic elements of a vacuum tube, showing the cathode, the anode, and a system of elements used to control the electron beam.

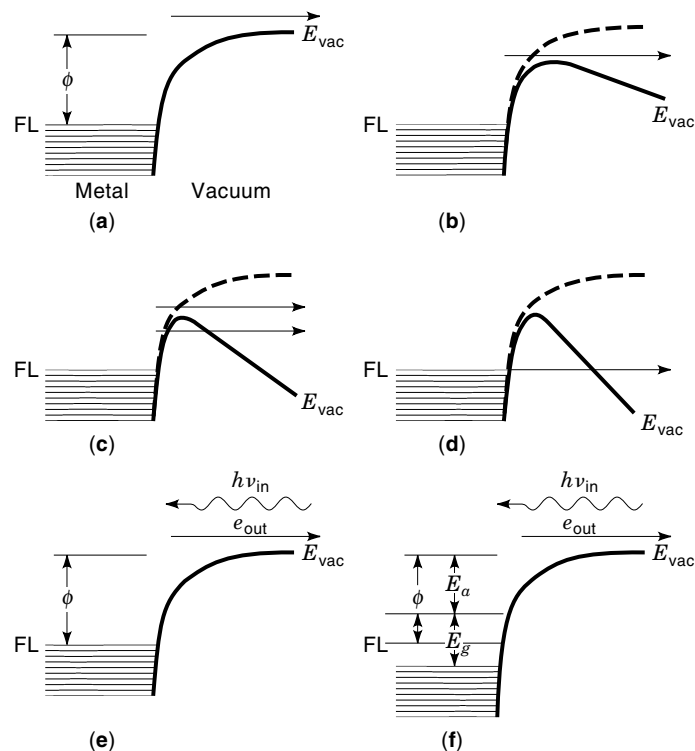


Figure 2. Potential energy diagrams illustrating the various methods of extracting electrons from a metal (a–e) and a semiconductor (e). Observe that the work function, ϕ , is the energy required to remove an electron from the Fermi level (FL) to the vacuum level E_{vac} . Electron emission occurs by two basic mechanisms, the excitation of electrons to energies above the vacuum level and by quantum mechanical tunneling. As shown, emission occurs as (a) Thermionic emission at low electric field; (b) Schottky emission, in which a moderate electric field at the surface of the thermal emitter lowered the energy barrier; (c) Thermal-field emission, in which electrons are emitted both thermally and by quantum mechanical tunneling through the barrier; (d) Field emission by tunneling at very high electric fields, but at low temperature; (e) Photoemission from a metal, resulting when an incident photon transfers its energy to an electron in the conduction band; and (f) Photoemission from a semiconductor occurs as electrons are ejected from the valence band at low temperature.

applications are being found for which existing cathodes are no longer adequate, calling for smaller dimensions, higher spatial resolution, greater currents, higher current densities, increased beam brightness, higher power, greater resistance to poisoning, longer life, higher frequency response, and greater stability. Demands for improved cathode performance assure a continuing search for new and better cathodes.

To understand electron emission, it is useful to think of the cathode as a potential energy box containing a pool of electrons (see Fig. 2). The potential outside the box is called the vacuum potential. For an electron to be liberated from the box, it must either be given enough energy to raise it to the vacuum level or it must find a way to tunnel directly from the cathode into vacuum. The energy required to raise an electron from the surface of the pool to the vacuum level is defined as the work function. In general terms, cathodic emission of electrons may be promoted thermally (thermionic emission, Fig. 2(b)), by the application of a high electric field (field emis-

sion, Fig. 2(d)), a combination of thermal and field (thermal-field emission, Fig. 2(c)), by the absorption of electromagnetic energy (photoelectric emission, Fig. 2(e)) or by the interactions with energetic electrons or ions incident on the cathode surface (secondary emission). The various modes of electron emission are illustrated by the potential energy diagrams shown in Fig. 2. As this figure shows, cathode performance is governed by three factors: work function, temperature, and the intensity of the electric field at its surface.

Thermionic cathode design was advanced considerably by the introduction, in 1950, of the barium oxide dispenser cathode. Since that time, a number of important improvements have been made in the design of the dispenser cathode so that, in spite of some of its shortcomings, it is currently the cathode of choice in many applications, including cathode ray and microwave tubes. A more recent development, the lanthanum hexaboride thermionic cathode, is now finding wide application in such devices as electron microscopes and scanning Auger microprobes.

Field emission cathodes, studied extensively during the 1950s and 1960s, have found application in electron optical systems and scanning tunneling microscopy. In recent years, the multiple-needle field emission cathode, consisting of a two-dimensional array of closely packed field emission tips, has begun to attract interest as an electron source in flat panel displays and microwave amplifiers. With its ability to deliver high current density, high brightness beams, the thermal-field cathode is finding application in systems requiring finely focused beams, such as electron-beam-lithography systems, electron microscopes, Auger electron spectrometers, and other electron microprobe systems.

Great strides were made during the decade of the 1960s in developing very efficient photocathodes that are now used extensively in photoelectronic optical systems such as photomultipliers, video cameras, and other image converting devices. Performance of these cathodes is quite remarkable, and very high current densities have been achieved.

Two highly experimental cathodes are worth considering for the fact that they are cold emitters and potentially capable of emitting high currents. The first employs techniques that were developed for the microelectronic industry to fabricate an entirely new class of cold electron emitters known as avalanche and metal–semiconductor–metal (MSM) cathodes. Still in the developmental stage, these cathodes are multilayer structures that are capable of emitting electrons by quantum tunneling at room temperature. The second takes advantage of the large currents generated in a plasma or glow discharge. By extracting the electrons from the ions in the plasma these cathodes are capable of producing high currents.

It is almost certain that further developments in electron beam devices will impose requirements that existing cathodes are unable to deliver. To the degree that this is true, there will be a continuing need for research directed toward the development of improved cathodes. In the following sections the basic theory of electron emission will be given, followed by a brief overview of common cathode materials, along with a brief discussion of the state of the art of practical cathodes.

THEORY

Thermal-Field Emission

In general, electron emission from a metal cathode surface depends upon three physical conditions, the work function, ϕ

Table 1. Current Density Equations for Thermal-Field Emission of Electrons

Regime	Temperature-Field Range	Current Density, (A/cm ²)	Eq. No
Thermionic Emission	(low F , high T)	$J_T = 120T^2 \exp\left(-1.16 \times 10^4 \frac{\phi}{T}\right)$ (Richardson–Dushman equation)	(2)
Schottky Emission	($F \leq 160T^{1.33}$)	$J_S = 120T^2 \exp\left[\frac{-1.16 \times 10^4 \phi(1-y)}{T}\right]$ (Schottky equation)	(3)
Extended Schottky Emission	($160T^{1.33} \leq F \leq 1100T^{1.33}$)	$J_{ES} = J_S \frac{\pi q}{\sin(\pi q)}$	(4)
Field Emission	($F \geq 9400\phi^{0.5}T$)	$J_{FE} = \frac{1.54 \times 10^{-6} F^2}{\phi t^2(y)} \exp\left[\frac{-6.83 \times 10^7 \phi^{1.5} v(y)}{F}\right]$ (Fowler–Nordheim equation)	(5)
Thermal-Field Emission	($9400\phi^{0.5}T \leq F \leq 4 \times 10^4 \phi^{0.5}T$)	$J_{TF} = J_F \frac{\pi p}{\sin(\pi p)}$	(6)

In these equations, the current density, J , has units of A/cm² when ϕ is measured in eV, F is in V/cm and T is in K. The parameters appearing in the equations are defined as:

$$y = 3.79 \times 10^{-4} \frac{\sqrt{F}}{\phi}$$

$$q = 5.04 \times 10^{-3} \frac{F^{0.75}}{T}$$

$$p = 8840 \frac{T\sqrt{\phi}t(y)}{F}$$

$$t(y) = 0.9967 + 0.716y + 0.0443y^2$$

$$v(y) = 1.10138 - 0.2676y + 0.7555y^2$$

(eV), the temperature, T (K), and the electric field intensity, F (V/cm). Electron emission is described customarily in terms associated with various ranges of temperature and field as illustrated in Fig. 2. Thermionic emission (TE) occurs at low fields and at temperatures sufficiently high to promote metallic electrons to energies above the vacuum level. In Schottky emission (SE), electrons are thermally emitted above a potential barrier that is lowered by an applied electric field. As higher electric fields, the potential barrier may be made thin enough for emission to occur as a combination of thermionic emission above the barrier and tunneling through the barrier, a process known as thermal-field emission (TFE). Field emission (FE) occurs at low temperature by tunneling through a potential barrier made quite thin by a very high electric field at the cathode surface. Photoelectric emission (PE), promoted by the absorption of photons incident on the cathode surface, is also strongly affected by temperature and electric field intensity. Secondary emission cathodes have been omitted from this article.

Theoretical analyses of electron emission over a wide range of temperatures and fields have been reviewed in a concise manner by Swanson and Bell (1). For more detailed treatments, the reader will want to consult reviews by Nottingham on thermionic emission (2) and by Good and Muller on field emission (3). In general, the current density of electrons emitted into a vacuum from a metal surface, in the absence of photon interactions, may be expressed by the integral equation,

$$J = e \int_W N(W)D(W) dW \quad (1)$$

where $N(W)$ is the number of electrons per unit energy arriving at the cathode–vacuum interface from inside the metal and $D(W)$ is the transmission probability. An analytical solution of Eq. (1) does not seem possible over the entire range of temperatures and fields; however, approximate solutions may be obtained for particular ranges of temperature and field and these are presented in Table 1. Temperature-field domains over which these solutions are valid are illustrated in Fig. 3.

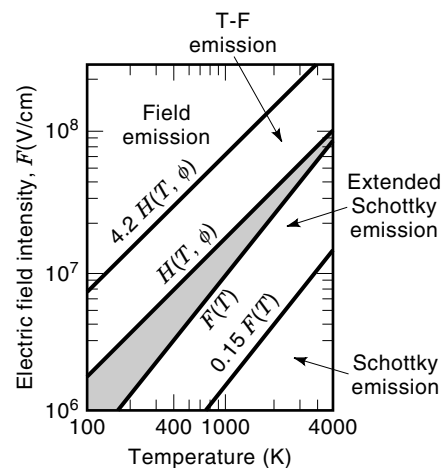


Figure 3. Various emission domains shown in terms of the electric field intensity at the surface of the emitter and the temperature.

Photoemission

Photoemission occurs by the ejection of electrons from either states at the surface of a material, or from states lying within its interior, by energy transferred from an incident photon. An in-depth discussion of photoemission from solids will be found in the work edited by M. Cardona (4).

The fundamental requirement for photoemission is that the energy given to the electron by the incident photon be sufficient to excite it from the Fermi level to the vacuum level [Fig. 2(e)]. In the case of emission from a metal at absolute zero, the excess photon energy is converted to kinetic energy of the emitted electrons according to the equation

$$E_e = h\nu - e\phi \quad (2)$$

where ν is the frequency of the incident photons. In the case of photoemission from a semiconductor at low temperatures [Fig. 2(f)], it is necessary for the incident electron to be excited from the valence band to the vacuum level, usually expressed in terms of the energy of the band gap, E_g plus the electron affinity E_a , in which Eq. (2) must be written as:

$$E_e = h\nu - (E_g + E_a) \quad (3)$$

At a temperature above absolute zero, electrons may be ejected from states above the Fermi level for metals and form the conduction band for semiconductors. This has the effect of making the threshold for emission less sharp.

To determine the photo-electron yield for a metal, one replaces the supply function $N(W)$ in Eq. (1) by

$$N(W + h\nu) = \alpha Z(h\nu)N(W) \quad (4)$$

where $Z(h\nu)$ is the probability that an electron will be excited from a state W to a state $W + h\nu$ and α is a cross section (of the order of 10^{-32} cm²-s/photon) for the excitation of a conduction electron by an absorbed photon. With this change, integration of Eq. (1) gives the current density of photo-emitted electrons as,

$$J_p = 120\alpha I(\nu)T^2 f(x) \quad (\text{A/cm}^2) \quad (5)$$

where $f(x)$ is a monotonically increasing universal function of the variable,

$$x = \frac{h(\nu - \nu_0)}{kT} \quad (6)$$

and $I(\nu)$ is the incident light intensity in photons/cm²-s. The function $f(x)$, is given by,

$$\begin{aligned} f(x) &= e^x - \frac{e^{2x}}{2^2} + \frac{e^{3x}}{3^2} - \dots & (x \leq 0) \\ &= \frac{\pi^2}{6} + \frac{x^2}{2} - \left[e^{-x} - \frac{e^{-2x}}{2^2} + \frac{e^{-3x}}{3^2} - \dots \right] & (x \geq 0) \end{aligned} \quad (7)$$

It is customary to present photo-electric data in the form of the so-called Fowler equation,

$$\log\left(\frac{J_p}{I(\nu)T^2}\right) = B + f(x) \quad (8)$$

These equations have all been derived for the case in which the applied electric field is zero. Extending the theory of photo-emission to include the effect of electric field reveals two important points: First, unlike the case of thermal emission, Schottky lowering of the potential barrier is not significant in photo-emission and second, photo enhanced field emission is possible, a fact that has been used to advantage in investigating surface states and surface band structure (5). Because of its limited practical application at the present time, photo-field emission will not be considered further in this article.

Space Charge

A theory of cathodes would be incomplete without at least a brief mention of space charge. In simple terms, electrons arrive at the surface of an electron emitter with kinetic energy of only a few electron volts. Although they are generally subject to an accelerating electric field, these electrons may still linger sufficiently long in the vicinity of the cathode surface to form, in effect, a negative charge layer near the surface. The presence of this space charge layer serves to reduce the electric field at the cathode surface and may even produce a negative potential gradient that inhibits further emission of electrons. In general, space charge depends upon electrode geometry, the current density at the cathode surface and the electric potential, all of which are interrelated in complex ways.

Space charge theory is derived from a solution of Poisson's equation:

$$\nabla^2\phi = -\frac{\rho}{\epsilon_0} \quad (9)$$

where ϕ is the electric potential in V and ρ is the electric charge density in the cathode-anode region in C/m³. Equation (9) may be solved to yield,

$$(2KJV^{1/2} - F_0^2)(4KJV^{1/2} + F_0^2)^{1/2} = 6K^2J^2d - F_0^3 \quad (10)$$

where, $K = \epsilon_0 \sqrt{(2e/m)}$, J and F_0 are, respectively, the current density and electric field at the emitting surface, and V is the cathode-anode potential difference (6). Here, in SI units, m is the electron mass and e is the electronic charge.

The electric field at the surface of the emitter is dependent upon V but the relationship is complex because of space charge effects that ensure that F_0 also depends on J . This consideration is important for emission domains in which the electric field is a significant factor; however, for thermionic emission in which F_0 is small, Eq. (10) reduces to the familiar Child-Langmuir (C-L) law:

$$J_C = \frac{4V^{3/2}}{9Ks} = 2.330 \times 10^{-6} \frac{V^{3/2}}{s} \quad (11)$$

In this expression, s is a parameter that depends on geometry with units of cm². For all but the simplest of configurations, the parameter, s , is a complicated function of the electrode geometry; however, values for a few common electrode configurations are presented in Table 2.

In the case of Schottky emission, the presence of space charge may be quickly recognized by plotting the current density as a function of the applied voltage on a log-log graph.

Table 2. Approximate Values of the s -Parameter for Various Cathode-Anode Configurations

Geometry	Defining Dimensions	s
Planar	Cathode-anode distance = d	d^2
Cylindrical		
Internal cathode	$3 \leq r_a/r_c < 10$	$\sim 0.144r_a^2(r_a/r_c)^{1.509}10^{-[\log(r_a/r_c)^{0.824}]^2}$
Internal cathode	$r_a/r_c > 10$	$\sim r_a r_c$
Spherical		
Internal cathode	$3 < r_a/r_c < 100$	$\sim r_c^2[-0.340 + 2 \log(r_a/r_c)]$

The resulting graph shows two regions, defined by $J_C < J_S$ (space charge limited or Child region) in which the graph has a slope of $3/2$, and $J_C > J_S$ (temperature limited or Schottky region), characterized by a nearly zero slope. This effect is illustrated in Fig. 4. Note that cathodes operating in the Child region are not dependent upon the work function. Readers are directed to the literature (7) for treatments of space charge for the case of field emission.

CATHODE MATERIALS

Practical cathode design is primarily a problem in materials science. While it is clear that a low work function is necessary to achieve the greatest emission current, a real cathode must also exhibit a number of other important characteristics, including a low rate of evaporation at the operating temperature, a high resistance to contamination and poisoning, a strong resistance to sputtering, thermal stability, mechanical durability, and in the case of photocathodes, a high quantum yield. As knowledge of materials science increases, it is possible to envision a time when cathodes will be purposefully engineered to possess the desired characteristics (low work function, low vaporization, chemical inertness, hardness, etc.) by creating exotic alloys or modifying the emitting surface by ion implantation. To some degree, this is the approach taken by the developers of thermionic dispenser cathodes and photocathodes in which the emitting surfaces are carefully modified by certain work function-lowering compounds or alloys.

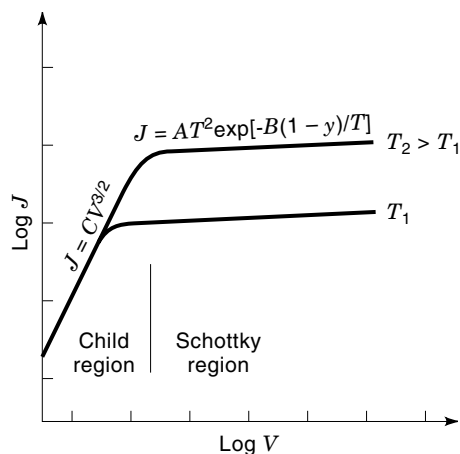


Figure 4. Schottky plots for a hypothetical thermionic cathode, showing the space charge limited (Child) and the temperature limited (Schottky) regions.

Cathode Material Characteristics

Thermionic cathodes are often characterized by plotting current density against the evaporation rate. Another useful way to characterize a thermionic cathode material is to define a figure of merit based on the Richardson equation:

$$\alpha = 2 \log T_m - 5 \times 10^3 \phi / T_m \quad (12)$$

in which the evaporation rate is roughly correlated with the melting temperature, T_m . Table 3 gives values of α for a few promising thermionic cathode materials.

The list of materials used as field emitters is comparatively much smaller than those used for thermionic cathodes. In general, practitioners in field emission have looked to the refractory metals or compounds for use as field emission cath-

Table 3. Figures of Merit for Some Thermionic Cathode Materials

Material	$\langle \phi \rangle$ (eV)	T_m (K)	α
Oxides			
CaO	1.8	2840	3.7
SrO	1.4	2700	4.3
BaO (on tungsten)	2.1	2190	1.9
BaO (on irridium)	1.5	2190	3.3
ThO	2.8	3460	3.0
Borides			
LaB ₆	2.7	2800	2.1
LaB ₆ (310) plane	2.4	2800	2.6
CeB ₆	2.7	2560	1.5
YB ₄	2.6	3070	2.7
GdB ₄	2.0	2920	3.5
Carbides			
TiC	3.3	3430	2.3
ZrC	3.4	3800	2.7
ZrC (210) plane	3.3	3800	2.8
NbC	3.5	3920	2.7
HfC	3.4	4160	3.2
TaC	3.6	4150	2.9
CeC ₂	2.5	2810	2.4
Metals			
Al	3.0	933	-10
Ba	2.5	1123	-10
C	4.7	3770	0.9
Cs	1.8	302	-25
Hf	3.6	2500	-0.4
Ir	5.4	2720	-3.1
Mo	4.3	2895	-0.5
Ta	4.1	3293	0.8
W	4.5	3695	1.0

Table 4. Most Commonly Used Materials for Field Emission Cathodes

Material	f (eV)	T_m (K)	Application
Tungsten	4.5	3695	most widely used
Molybdenum	4.3	2895	field emitter arrays
Silicon	4.85	1687	field emitter arrays
	$E_g + E_a = 4.15$		
W-Zr-O	2.5-2.7		Schottky/T-F emitters
W-Hf-O	2.7		Schottky/T-F emitters
LaB ₆	2.4	2800	Cold and Schottky emitters
ZrC	3.4	3800	
HfC	3.4	4160	

odes because of their high thermal and electrical conductivity and their resistance to vacuum arc and sputtering damage by back-streaming ions. Materials that are most frequently used as field emission cathodes are listed in Table 4.

A complete listing of materials used as photocathodes is far too extensive to include here. Suffice it to say, photocathode development has become a very sophisticated science. The major considerations are the work function for metals, the energy band gap, E_g , and electron affinity, E_a , for semiconductors and the quantum efficiency, Q in emitted electrons per incident photon. The properties of a few practical photocathodes are presented in Table 5. An extensive review of photocathodes has been published by Sommer (8).

Negative Electron Affinity Materials

Because of their application in photo and tunnel cathodes, it is important to call attention to a class of materials that have negative electron affinity (NEA). A NEA material is a semiconductor in which the conduction band edge lies above the vacuum level. First observed in the 1960s, NEA is achieved by modifying the surface of a semiconductor in order to lower the vacuum level relative to the conduction band edge. This is usually done by the adsorption of a thin film of a low work function material onto a p -type semiconducting surface. In principle, NEA is achieved when the work function of the adsorbed layer is less than the band gap energy.

Table 5. Properties of a Few Practical Photocathodes

S-number	Cathode Material	$E_g + E_a$ or ϕ (eV)	Wavelength at Peak Sensitivity λ_p (nm)	Quantum Yield at λ_p
S-1	Ag-O-Cs		800	0.005
S-10	Bi-Ag-O-Cs	1.6	400	0.10
S-11	Cs ₃ Sb	2.1	450	0.20
S-20	Cs-Na ₂ KSb	1.5	400	0.30
	K ₂ CsSb	2.1	400	0.30
	K ₂ CsSbO	<2.1	400	0.35
	LaB ₆	$\phi = 2.7$		0.0001
	GaAs(Cs-O)	$E_a < 0$	860	0.17
	InGaAs(Cs-O)	$E_a < 0$	1000	0.0015
	Si(100)-Cs-O	$E_a < 0$		

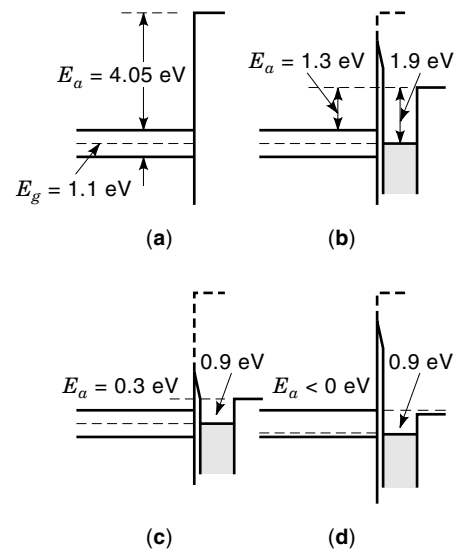


Figure 5. Potential energy diagrams illustrating the conversion of the (100) plane of silicon from a normal electron affinity to negative electron affinity surface. Adsorbing a layer of cesium onto a clean, undoped silicon surface, (a) Will have the effect of reducing the electron affinity to 1.3 eV, (b) By co-adsorbing a layer of oxygen the electron affinity is further reduced to 0.3 eV. (c) Repeating steps (a-c) for strongly p -doped silicon results in a negative electron affinity (9).

In the simplest possible terms, this method of achieving NEA is illustrated in Fig. 5, using Si as an example. The (100) crystal plane of silicon has an energy band gap of 1.1 eV and an electron affinity of about 4.0 eV as shown in Fig. 5(a). In Fig. 5(b), adsorption of a layer of Cs, with a work function of 1.9 eV, effectively reduces the electron affinity to about 1.2 eV. Activating the cesium surface with oxygen reduces the electron affinity yet further to 0.9 eV, as shown in Fig. 5(c). Then, as illustrated in Fig. 5(d), strong p -doping of the silicon brings the Fermi level near the valence band edge, giving an electron affinity of less than 0 eV. It is possible to obtain NEA by this method for the (100) plane of silicon but not other orientations. One example of a NEA surface has been reported by Santos and MacDonald (10).

THERMIONIC CATHODES

Basic Considerations

Historically, the electronics industry was founded upon the use of vacuum tubes powered almost entirely by thermionic cathodes. Even today, thermionic cathodes are the electron sources of choice in the vast majority of vacuum electronic devices now in service, including cathode ray tubes, microwave amplifiers, x-ray sources, and the various specialty vacuum tubes used in electronic circuits. The practical attractiveness of the thermionic cathode lies in the ease with which it may be mass produced, its reliability, and its long life. Of the thermionic cathodes in service, the dispenser cathodes are the most commonly used. Excellent reviews by Thomas et al. (11), Cronin (12), and Shroff and co-workers (13) cover the state of the art of dispenser cathodes.

The Dispenser Cathodes

Definitions. Table 3 shows that Group I and II metal oxides have high figures of merit; however, because they tend to be structurally weak and evaporate rather quickly at operating temperatures, they are customarily used as dispenser cathodes. Dispenser cathodes have been designed to compensate for evaporation by ensuring a constant supply of oxide. A typical dispenser cathode is shown schematically in Fig. 6. Since the introduction of the L-type cathode in 1950, several types of dispenser cathodes have been developed. These are described as follows:

1. The L-type cathode is the first dispenser cathode used commercially. This cathode consists of a thin wafer of porous, sintered tungsten referred to as a matrix. Just behind the wafer is an oxide filled cavity that serves as a reservoir for dispensing the oxide. As the cathode is heated, oxide migrates through the matrix, coating the emitting surface with an oxide layer, which then reacts with the tungsten surface to create a Ba–O dipole layer, which in turn reduces the work function.
2. B-type: Instead of the cavity used in the L-type cathode, the B-type cathode, introduced in 1950, uses a sintered tungsten (or other metal) matrix that is impregnated with an oxide eutectic. During use, the impregnated oxide diffuses to the surface where it is activated to produce a thin low work function surface layer. The B-type cathodes are characterized by specifying the proportions of BaO:CaO:Al₂O₃ impregnant to be 5:3:2.
3. S-type: The S-type cathode is identical to the B-type but with a BaO:CaO:Al₂O₃ impregnant in the proportions 4:1:1.
4. M-type: Invented in 1966, this cathode is a B- or S-type cathode with a surface coating, or top layer, of osmium [M(Os)], ruthenium [M(Ru)], or iridium[M(Ir)]. At 1300 K, these cathodes generate three times the emission of the B-type cathode.
5. MM-type: Often referred to as a mixed matrix cathode, the MM-type cathode is made by mixing a second metal (Os, Ir, Ru) with the tungsten prior to sintering.
6. CMM-type: This is an osmium MM cathode coated with an additional surface layer of osmium.
7. CD-type: A standard dispenser cathode with an osmium-tungsten alloy substrate.

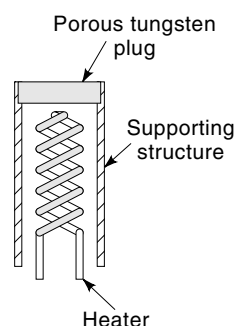


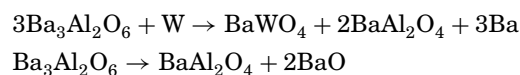
Figure 6. A typical dispenser cathode.

8. Scandate type: A mixed matrix cathode in which barium scandate is mixed with the tungsten powder prior to sintering. These cathodes are activated without further impregnation.

Other designs are continually being researched. For example, the controlled porosity dispenser uses a W–Os or W–Ir foil with tiny, closely spaced laser milled holes in it for the even dispersing of the oxide over the surface. Still other workers are investigating the use of thin layers of an alloy on the cathode surface.

B- and S-Type Cathodes. B- and S-type cathodes consist of an indirectly heated porous plug (matrix) made by sintering 4 mm tungsten powder to give a porosity of 17–20%. Impregnation is achieved by immersing the plug in a melt of the impregnant, which is usually a mixture of BaO·CaO·Al₂O₃ in the ratio of 5:3:2 (B-type) or 4:1:1 (S-type). These impregnants have been chosen to eliminate excessive Ba evaporation. Activation of the cathode to maximize emission is effected by heating in vacuum for several hours.

The mechanism for lowering the work function is complex and the electrical, kinetic, and chemical properties of these cathode systems are not completely understood. It does seem clear, however, that the cathodes are activated by chemical reactions occurring at the cathode surface. During activation, Ba and BaO are believed to be formed by the following reactions:



Following activation, a decrease in emission from dispenser cathodes is often observed over time. This is believed to be due to (1) The depletion of BaO on the emitting surface, (2) Poisoning of the cathode surface by exposure to oxygen and water vapor, (3) Poisoning by the deposition of anode material on the emitting surface (4) The migration of carbon to the emitting surface from within the bulk material, and (5) Sputtering by back streaming ions formed by the ionization of residual gases.

To achieve a current density of 40 A/cm² to 50 A/cm², a standard B- or S-type cathode would have to be operated at a temperature of 1770 K. At this temperature, the expected useful life would be only about 40 h. This limitation led to the development of the M and MM cathodes.

M- and MM-Type Cathodes. It is a well-known fact that the higher the work function of the refractory metal substrate the lower the minimal attainable work function produced by the adsorption of Group I and II metal oxides adsorbates on that substrate. This fact has been used to advantage in dispenser cathode design and has led to the development of the M- and MM-type cathodes. In the M-type cathode, a noble metal (Os, Ir, Ru), having a relatively high work function, is evaporated as a top layer onto a standard B-type structure. In the MM-type, or mixed matrix, cathode, noble metal powder is mixed with the tungsten prior to sintering to form the porous base.

Scandate Cathodes. A scandate cathode is a mixed matrix cathode in which barium scandate is mixed with the tungsten powder prior to pressing to produce the metal substrate.

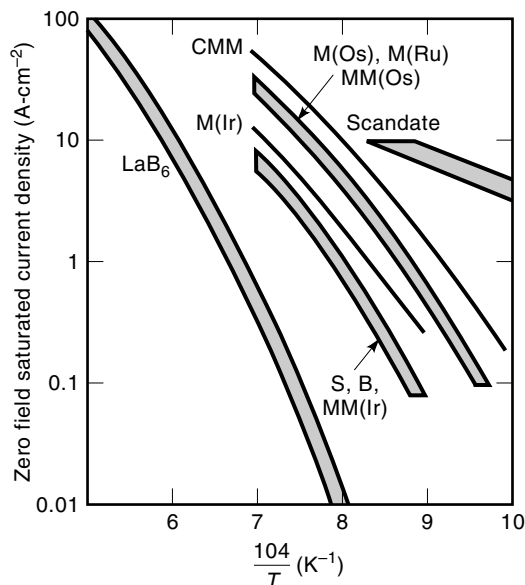


Figure 7. Richardson plots comparing the performances of a number of dispenser (B, S, M, MM, CMM) and LaB_6 thermionic cathodes.

These cathodes, activated without further impregnation have excellent emission properties, low evaporation, long life, a work function of 1.78 eV at 1220 K, and yield current densities as high as 100 A/cm^2 .

Boride Cathodes

Certain rare-earth metal borides are known to have excellent emission properties. The most commonly used are LaB_6 and CeB_6 whose work functions are about 2.7 eV. The highest current density is obtained from LaB_6 . With a figure of merit of around 2.1 (Table 3), LaB_6 would appear to be only moderately favorable as a cathode material in comparison with the Group I and Group II oxides. However, because of its higher melting temperature and lower evaporation rate, it has been possible to obtain current densities of 100 A/cm^2 LaB_6 cathodes. Furthermore, LaB_6 is very robust in comparison to the oxides, accounting for the considerable attention it has received as a cathode material, particularly in focused beam applications. The chief reason that the LaB_6 cathode has not been used more widely is the higher heating power required.

Figure 7 compares emission characteristics of the various types of thermionic cathodes (B, S, M, MM, CMM, scandate, and LaB_6).

FIELD EMISSION CATHODES

Basic Considerations

Field emission of electrons occurs by quantum mechanical tunneling through a potential barrier made narrow by an electric field of the order of 10 MV/cm . In order to achieve the required electric field intensities, it is customary to use a very sharply etched needle as the cathode. Field emission cathodes have a number of attractive features: They may be operated cold, which eliminates the need for a heating power source. Current densities as high as 10 MA/cm^2 have been obtained for dc operation and up to 0.1 nA/cm^2 for pulsed emission.

Being strongly field dependent, they may be switched on and off with frequencies as high as GHz. Since the emitted electrons emerge from the apex of a very sharp needle, field emission cathodes are essentially point sources. They exhibit extremely high brightness through the combination of high current density and small emitting surface. The last three characteristics make them especially well suited for use in electron optical systems.

Several characteristics of field emission cathodes have limited their application. First, field emission is strongly dependent on work functions making them extremely sensitive to the adsorption of residual gases in the vacuum chamber. Second, the strong dependence on the electric field can be a problem when sputtering of the emitter surface by back-streaming ions creates surface irregularities. These irregularities cause local field enhancement that results in unstable emission. Third, resistive heating at the emitter tip at high current densities may lead to a runaway condition that ends in a vacuum arc and destruction of the emitter. Finally, although emission current density may be quite high, total current is usually small because of the small emitting area, typically of the order of 10^{-8} cm^2 . In spite of the limitations, field emission cathodes are finding wide application in scanning tunneling electron microscopes (STEM) and scanning electron microscopes (SEM) and in the two-dimensional field emitter arrays used in certain flat-panel displays.

The physical properties most important for field emission cathodes are high thermal and electrical conductivity, a high melting temperature to permit the emitter to be cleaned thermally, a surface that is chemically inert, and a material that is resistant to sputtering by back-streaming ions. These requirements have restricted the choices to the refractory materials. Tungsten field emitters have been used extensively but, although it is quite refractory and has excellent thermal and electrical conductivity, a clean tungsten surface reacts readily with the residual gases in the vacuum and it is not very resistant to sputter damage. Recently, there has been considerable interest in using LaB_6 , ZrC, and HfC emitters in cold field emission applications. These materials have lower work functions, chemically less reactive surfaces, and they are more resistant to sputtering.

More information concerning the application of field emission may be found in the reviews by Dyke and Dolan (14) and Gomer (15), as well as those of Swanson and Bell (1) and Good and Muller (3).

Field Emitter Arrays

Because the total current from a single tip is quite small (of the order of $10 \text{ }\mu\text{A}$), high current field emission can only be realized by using arrays of multiple needles. However, this is not as simple as might at first be imagined because, as the emitters are brought near one another, the field at each emitter surface is reduced by the mutual shielding of the neighboring emitters. Thus, the total current is determined by two competing factors: the linear increase in current with an increasing number of emitters and a reduction in current due to the shielding effect. The shielding effect may be avoided by providing each emitter with its own closely spaced anode, an approach taken in the design of the so-called Spindt cathode and its close relatives.

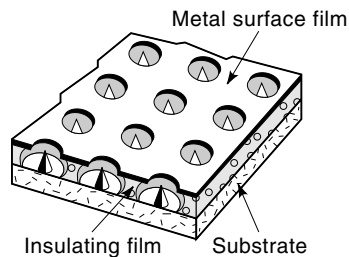


Figure 8. Spindt-type, multiple tip array, field emission cathode.

Spindt Cathode

Shown schematically in Fig. 8, the Spindt cathode consists of an array of metal cones (usually molybdenum) deposited by evaporation onto a silicon substrate. An important factor in the design of the Spindt cathode is that each emitter is centered within a small aperture in a control grid, which eliminates the shielding effect of the other emitters. Spindt cathodes have been fabricated with packing densities as high as $5 \times 10^6/\text{cm}^2$ and cathodes with up to 40,000 individual emitters are made routinely. Because of the close proximity of the control grid, these cathodes operate at only a few hundred volts and at current densities of 50 A/cm^2 . Lifetimes in excess of 50,000 h can be expected under controlled conditions. Work is still ongoing in an effort to overcome the present limitations of the Spindt cathode. Other configurations, including wedges, are also being investigated. These and other issues are discussed in the excellent reviews of Iannazzo (16) and Forman (17).

EXTENDED SCHOTTKY AND THERMAL-FIELD CATHODES

Cathodes that operate in the extended Schottky (ES) and thermal-field (TF) modes are discussed together, since the transition from one to the other is continuous, depending upon the particular values of the applied electric field and temperature (Fig. 9). Often, these terms are used inter-

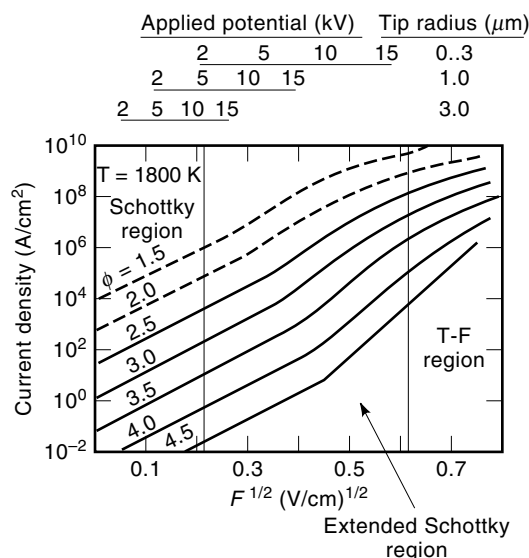


Figure 9. Schottky plots for a Schottky-TF emission cathode for different work functions and tip radii. A temperature of 1800 K is assumed in all cases.

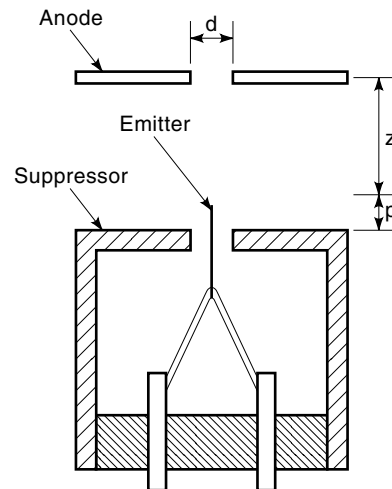


Figure 10. Schematic drawing of a Schottky cathode.

changeably. Cathodes operating in the ES mode are the dominant electron source in focused electron optical devices, that require high brightness, high angular intensity, low energy spread, low noise, and long life. Prominent applications include e-beam lithography systems, electron microscopes, micro-electronic, and Auger microprobes. The most commonly used TF cathode is the zirconiated (Zr/O/W) tungsten emitter, which is commonly arranged as shown in Fig. 10.

The performance of a TF emitter is determined by a combination of tip radius, electrode configuration, and the operating parameters, all of which are interdependent. The operating parameters, defining the operation of a TF cathode are the temperature T , the suppressor voltage V_s , and the extractor voltage, V_e . For a Zr/W/O, cathode operating at a temperature of 1800 K, V_s ranges between -1200 V and -300 V . The value of the extractor voltage is dependent upon the desired angular intensity, I' in A/sr . As an example, values for I' and V_e can be approximated for one commercial Zr/O/W cathode (FEI Co., Beaverton, OR) by the empirically derived formulas:

$$\Gamma = \frac{2.8 \times 10^{-25} V_e^{4.2}}{r^{1.1} z^{3.0}} \quad (13)$$

$$V_e = 6.9 \times 10^5 r^{0.27} z^{0.71} \Gamma^{0.24} \quad (14)$$

where V_e is in V, r , and z are in cm, and I' is in mA/sr . These expressions are valid for $4\text{kV} < V_e < 8\text{kV}$, $0.3 < r < 1 \mu\text{m}$, and $250 < z < 500 \mu\text{m}$. A good source for learning more about the TF cathode is the paper by Swanson and Tuggle (18).

PHOTOCATHODES

Photocathodes are used extensively in photomultipliers and various other photo-electronic imaging devices. In addition, considerable interest has been shown in the use of photo-emission to generate high current, high power electron beams for application in such devices as free electron lasers and gyratrons. Photocathodes offer several advantages over thermionic and field emission cathodes: (1) Heating or high electric fields are not required; (2) The electron beam may be easily modulated by modulating the incident light intensity; (3) The

shape and size of the cathode may be altered to suit the particular application; and (4) The energy spread of the electron beam is relatively small. Elimination of the need for heating simplifies the fabrication of cathode structures and reduces greatly cathode power requirements, for example, 6 J of photon energy per microsecond pulse as compared to 2500 W of heating power over a duration of minutes for a 16 cm² LaB₆ cathode.

Before reviewing the basic types of photo-emitters, it is helpful to present the basic photo-emission equation containing the quantum yield, Q , which is defined as the number of emitted electrons per incident photon. Using this definition of quantum yield, the emitted current density is given as

$$J_p = \frac{eI}{hv} Q(v) = 8 \times 10^5 \lambda I Q(v) \quad (\text{A/cm}^2) \quad (15)$$

where λ is the wavelength in meters and I is the intensity of the incident light in W/cm². With $Q = 10^{-3}$ and $\lambda = 0.532$ mm, this yields a current density of 100 A/cm² at an incident light power density of 230 kW/cm². The energy density in a 1 ms pulse is 230 mJ/cm².

The quantum yield depends on several factors: First, it depends on the surface and bulk electronic structure of the cathode, described in terms of the work function the band-gap energy and electron affinity. Second, the yield factor varies considerably from one cathode to the next, often displaying a maximum for wavelengths well below threshold. Third, the quantum yield will depend on temperature. Fourth, because the photon interaction often occurs at depths of a few hundred angstroms inside the cathode, the transmission of both the electron and the photon within the cathode material has a significant influence on the quantum yield. As an illustration, Fig. 11 shows the quantum yields for selected cathode materials plotted against wavelength.

Photo-emitters designed for high current applications must have three important characteristics: a low work function, relative insensitivity to the adsorption of residual gases, and the ability to withstand the high temperatures generated by absorption of the incident electromagnetic radiation and by resistive heating. For long-term operation, consideration must also be given to the fact that poisoning by adsorbed residual

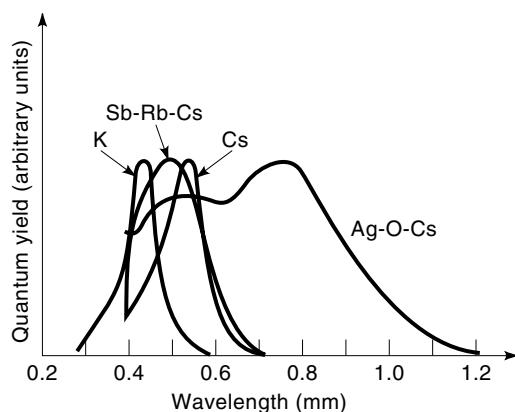


Figure 11. Relative quantum yields for four different photocathodes, showing differences in their spectral sensitivities. Quantum yields have been normalized to the same value.

gases and fatigue due to exposure to the incident light beam may lead to deterioration of the cathode with time.

A summary of photocathode characteristics is presented in Table 5. A few remarks about the different types of photocathodes follows.

Metal Photo-Emitters

Photo-emission from metals has been studied extensively (19). The emitting surface of most practical metal photocathodes consists of a thin oxide layer. Except for the alkali metals, these emitters are generally stable to environmental effects, but their energy thresholds are relatively high and their quantum efficiencies are low (10⁻⁴% to 10⁻³%). For these reasons the nonalkali metal photo-emitters are of limited usefulness. The alkali metals have narrowly peaked quantum efficiency curves in the visible spectrum but they are problematical because of their low vapor pressures.

Multi-Element Photo-Emitters

Multi-element semiconductor photocathodes are used widely in photo-electronic imaging devices. The most common of these are the so-called multi-alkali photocathodes of which Cs₃Sb, Na₂K₂Sb, Na₂K₂Sb(Cs), GaP(Cs), Ga(As, P)(CsO[F]), and GaAs(Cs, O[F]) are examples. All of the listed compounds either contain or are activated by an alkaline metal and they are all responsive to visible radiation. These compounds tend to decompose at high temperatures and they must be operated at pressures lower than 10 nPa. Quantum efficiencies for these cathodes lie in the range of 1% to 3% and as a result, quite high current densities have been reported. For example, current densities in excess of 600 A/cm² have been reported for Cs₃Sb cathodes in 60 ps pulses at acceleration potential differences of 1 MeV. Large pulsed currents have also been produced from GaAs(Cs, O) at the Stanford Linear Accelerator.

LaB₆ Photo-Emitters

The lanthanum hexaboride cathode surface seems to be more tolerant to the presence of oxygen than other photocathodes and this cathode may be operated under poorer vacuum conditions and at higher temperatures than the semiconductor photo-emitters. They may be made quite large. Photocathodes made of LaB₆ typically exhibit quantum efficiencies on the order of 10⁻²% when irradiated with radiation of wavelength of 308 nm.

Negative Electron Affinity Photo-Emitters

In recent years, certain NEA photo-emitters have attracted attention. The most prominent of these are the Si(100)(Cs-O) and GaAs(CS-O) NEA photocathodes. Quantum efficiencies for these cathodes are relatively high, with GaAs(CS-O) having a quantum efficiency of 17% and they have high spectral sensitivities in the infrared frequency range. Erjavec (20) has summarized the properties of these emitters.

THIN FILM TUNNEL CATHODES

Metal-Semiconductor-Metal Cathode

Several schemes have been proposed for the fabrication of cold electron emitters using techniques developed by the

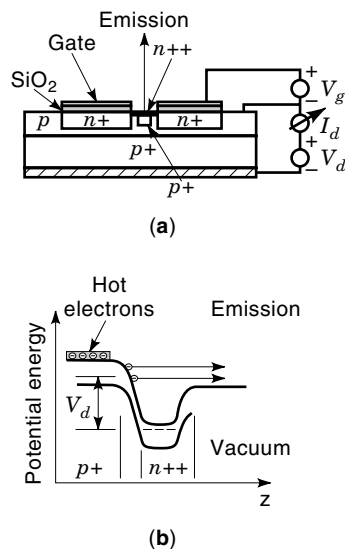


Figure 12. Van Gorkom-Hoeberechts avalanche tunnel diode. (a) Cross section. (b) Potential energy diagram.

semiconductor electronics industry. In one way or another, these schemes rely upon quantum tunneling to extract electrons from a thin film structure. Because of the experimental nature of these cathodes they will only be introduced briefly here. Many of the basic concepts governing the operation of the tunnel cathodes can be illustrated by considering two types of cathode, the avalanche and the metal-semiconductor-metal (MSM) cathode. The interested reader will find a more in-depth review of the subject in Ref. 21.

Avalanche Diode Emitter

Electron emission from a reverse biased silicon $p-n$ junction was first reported in 1957. Research conducted since that time has led to the development by van Gorkom and Hoeberechts (22) of a practical avalanche $p-n$ junction cathode. Emitters based on this principle are capable of delivering current densities of up to 8000 A/cm^2 into a vacuum from a spot size of $3 \mu\text{m}$ or less. High brightness is another feature of these cathodes, being approximately $9 \text{ MA/cm}^2\text{sr}$ (at 10 kV). A larger emitting area is possible but at the expense of current density. The long-term stability of the emission is surprisingly good, in spite of adsorption of oxidizing gases from the vacuum. Besides their very high current density and brightness, avalanche cathodes have other desirable features: they are easily and rapidly modulated, they use little energy, and they are relatively easy to manufacture, using techniques common to the microelectronic industry.

A schematic of the Van Gorkom and Hoeberechts avalanche diode is shown in Fig. 12. Electron emission occurs from an area in which an avalanche breakdown is created by the strong electric field produced at a reverse-biased $p-n$ junction. The emission characteristics depend mainly on the geometry, the doping and the purity of the surface. The best results are obtained with cathodes that have a very shallow $p-n$ junction (about 10 nm below the surface) and a very small emitting area. Emission is enhanced by coating the emitting surface with a monolayer of cesium, yielding an emission efficiency of up to 5% . Electrons are emitted essen-

tially as hot electrons with an effective electron temperature of as high as 5700 K . As shown in Fig. 12(b), electrons tunnel from a p^+ region through a very thin n^{++} layer directly into vacuum. Although the energy spread of the emitted electrons amounts to 1.2 eV , the aperture acts as an energy selector to limit the spread of the emitted beam to about 0.35 eV .

The small dimensions of the avalanche cathode means that very fast switching of the emission current is possible. The fast writing times possible and the ability to produce arrays of these cathodes makes them suitable for use in electron lithography systems and flat panel displays.

Metal-Semiconductor-Metal Cathode

Cold emission can also be realized by tunneling through a thin insulating or semiconducting layer sandwiched between two metal layers, the metal substrate and a metal surface layer. These cathodes are referred to respectively as metal-insulator-metal (MIM) and metal-semiconductor-metal (MSM) cathodes. For emission to occur, the insulator and surface layer must be very thin and emission is enhanced if the surface layer has a low work function. The development of the MIM cathode had its beginning in 1961 when Mead demonstrated the feasibility of cold electron emission into vacuum from a layered metal-insulator-metal device. In these devices, the insulating and surface films are a few tens of angstroms in thickness. Electrons thus injected into the conduction band of the insulator are accelerated by the strong electric field in the film, acquiring sufficient energy to escape through the metal surface film into the vacuum. Current densities of a few milliamperes per square centimeter are typically observed, with emission efficiency below 1% . Interestingly, the transfer ratio may be significantly improved by depositing a low work function layer as the metallic surface film.

In general, the performance of the early MIM cathodes was not spectacular, which undoubtedly explains why they attracted so little attention in ensuing years. Nonuniform emission, noise, and electrical breakdown are limiting characteristics but the more serious short-coming of these cathodes is the disappointingly low transfer ratio for emission. Replacement of the insulator with a wide band-gap, low (or negative) electron affinity semiconductor has been proposed as a way to overcome some of the problems of the MIM cathode. The use of a wide band semiconductor offers the possibility of engineering the band-gap to overcome some of the disadvantages of the earlier devices. As illustrated in Fig. 13, an ohmic contact may be formed at the substrate-semiconductor interface

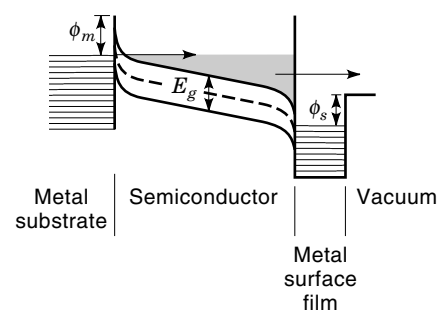


Figure 13. Energy diagram for a metal-semiconductor-metal, negative electron affinity tunnel cathode.

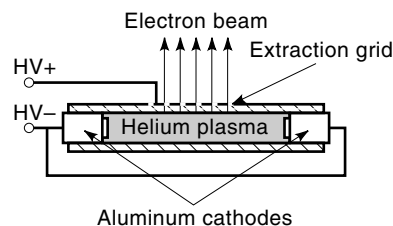


Figure 14. Reflex glow-discharge electron source.

by n -doping the semiconductor, enhancing the injection of electrons from the metal substrate into the conduction band. At the same time, heavy p^{++} doping at the semiconductor-surface metal interface pulls the band edges down, creating a low (or negative) electron affinity interface with the vacuum.

This approach is similar to that used in creating negative electron affinity photocathodes but here, the use of a narrow band-gap semiconductor is unnecessary because of direct injection of electrons into the conduction band. This distinction means that MSM cathodes are free from some of the restrictions that have persistently plagued photocathodes. For example, the use of a wide band-gap semiconductor permits the use of higher work function surface films than those required of photocathodes. This offers a wider selection of materials for these films, including films that are known to have a high resistance to contamination. Two other reasons for looking to wide band-gap materials is that they will sustain higher internal fields before breakdown and they offer the possibility of loss-free acceleration of electrons to energies well above the vacuum level of most metals. There is yet much work to be done before these cathodes will be of practical importance.

PLASMA ELECTRON EMITTERS

Plasmas are rich sources of electrons. A plasma cutting torch, for example, operates at currents as high as 300 A in air. That plasmas have been ignored as sources of electron beams is most likely because of the inherent difficulties of separating the electrons from the ions in the plasma. Also, they are not easily adapted to applications requiring vacuum. However, a number of workers have successfully extracted electrons from a glow discharge, making possible the generation of large area emission of electrons at relatively high current densities. An example of such a cathode is one developed by Murray and co-workers (23) shown in Fig. 14. This source consists of two opposed cylindrical aluminum cathodes 3 cm in diameter and separated by a distance of 15 cm. At a distance midway between the two cathodes, two grids are placed with their surfaces parallel to but displaced from the cathode axis. The purpose of these grids is to extract the electrons from the plasma created in the space between the cathodes.

In operation, both cathodes are held at the same potential. A helium pressure of 26.7 Pa is maintained in the space between the cathodes. The grids are held at a potential several kilovolts more positive than the cathodes. Thus, electrons leaving the cathode surface are accelerated into the cavity, creating a glow discharge. Because the mean free path of the electrons is several times the dimensions of the cavity, the electrons oscillate back and forth several times in the space between cathodes before they dissipate their energy in ioniz-

ing and exciting collisions with the helium atoms. As they give up their energy, the electrons approach thermal equilibrium with the plasma. The effect of this motion is to create an almost electric field free plasma in which the secondary electrons created by ionization thermalize to a very low electron temperature (<1 eV). Electron currents in excess of 100 A (current density equal to >10 A/cm²) may be extracted from the plasma in 10 ms pulses and accelerated to energies greater than 1 keV in the gap between the two grids.

BIBLIOGRAPHY

1. L. W. Swanson and A. E. Bell, Recent advances in field electron microscopy of metals, *Advan. Electron. Electron Phys.*, **32**: 193–309, 1973.
2. W. B. Nottingham, Thermionic emission, in S. Flügge (ed.), *Handbuch der Physik*, **XXI**, Berlin: Springer-Verlag, 1956, pp. 1–175.
3. R. H. Good, Jr. and E. W. Muller, Field emission, in S. Flügge (ed.), *Handbuch der Physik*, **XXI**, Berlin: Springer-Verlag, 1956, pp. 176–231.
4. M. Cardona (ed.), *Photoemission in Solids, I: General Principles*, New York: Springer-Verlag, 1978.
5. P. J. Donders and M. J. G. Lee, Thermal field emission and thermal photofield emission from tungsten (110), *Surface Sci.* **175**: 197–214, 1986.
6. J. P. Barbour et al., Space-charge effects in field emission, *Phys. Rev.* **92** (1): 45–51, 1953.
7. Y. Y. Lau, Y. Liu, and R. K. Parker, Electron emission: from the Fowler-Nordheim relation to the Child-Langmuir law, *Phys. Plasmas*, **1** (6): 2082–2085, 1994. Additional articles cited in this reference.
8. A. H. Sommer, *Photoemissive Materials*, Melbourne: Krieger Publishing Company, 1980.
9. T. Guo, Negative electron affinity silicon heterojunction photocathodes with alkali antimonide intermediate layers, *J. Appl. Phys.* **72** (9): 4384–4389, 1992.
10. E. J. P. Santos and N. C. MacDonald, Selective emission of electrons from patterned negative electron affinity cathodes, *IEEE Trans. Electron Devices*, **41**: 607–611, 1994.
11. R. E. Thomas et al., Thermionic sources for high-brightness electron beams, *IEEE Trans. Electron Devices*, **37** (3): 850–861, 1990.
12. J. L. Cronin, Modern dispenser cathodes, *IEEE Proc. I, Solid-State and Elect. Dev.*, **128**: 19–32, 1981.
13. A. M. Shroff, P. Palluel, and J. C. Tonnerre, Performance and life tests of various types of impregnated cathodes, *Appl. Surface Sci.* **8**: 37–49, 1981.
14. W. P. Dyke and W. W. Dolan, Field emission, *Advan. Electron. Electron Phys.* **8**: 89, 1956.
15. R. Gomer, *Field Emission and Field Ionization*, Cambridge: Harvard University Press, 1961.
16. S. Iannazzo, A survey of the present status of vacuum microelectronics, *Solid-State Electron.*, **36** (3): 310–320, 1993.
17. R. Forman, Evaluation of the emission capabilities of Spindt-type field emitting cathodes, *Appl. Surface Sci.*, **16**: 277–291, 1983.
18. L. W. Swanson and D. Tuggle, Recent progress in thermal field electron source performance, *Appl. Surface Sci.*, **8**: 185–196, 1981.
19. G. L. Weissler, Photoionization in gases and photoelectric emission, in S. Flügge (ed.): *Handbuch der Physik*, **XXI**, Berlin, Springer-Verlag, 1956, pp. 305–382.
20. B. Erjavec, Photoemission from semiconductors, *Elektrotehniski Vestnik*, **59** (1): 6–14, 1992.

21. W. M. Feist, Cold electron emitters, *Advan. Electron. Electron Phys.* Supplement 4: 1–57, 1968.
22. G. P. van Gorkom and A. M. E. Hoeberechts, Performance of silicon cold cathodes, *J. Vac. Sci. Technol.*, **B 4** (1): 108–111, 1986.
23. C. S. Murray, J. J. Rocca, and B. Szapiro, A reflex electron beam discharge as a plasma source for electron beam generation, *IEEE Trans. Plasma Sci.*, **16**: 570–573, 1988.

C. H. HINRICHS
Linfield College

CATV. See CABLE TELEVISION SYSTEMS; METROPOLITAN
AREA NETWORKS.